International Journal of Modern Physics A
© World Scientific Publishing Company

arXiv:1702.01526v1 [hep-lat] 6 Feb 2017

# CONSTRUCTION OF LATTICE MÖBIUS DOMAIN WALL FERMIONS IN THE SCHRÖDINGER FUNCTIONAL SCHEME

YUKO MURAKAMI[1,b] and KEN-ICHI ISHIKAWA[1,2,a]

[1] *Graduate School of Science, Hiroshima University, Higashi-Hiroshima, Hiroshima 739-8526, Japan*

[2] *Core of Research for the Energetic Universe, Hiroshima University, Higashi-Hiroshima, Hiroshima 739-8526, Japan*

[a] *ishikawa@theo.phys.sci.hiroshima-u.ac.jp*

[b] *d152338@hiroshima-u.ac.jp*

In this paper we construct the Möbius domain wall fermions (MDWF) in the Schrödinger functional (SF) scheme for the SU(3) gauge theory by adding a boundary operator at the temporal boundary of the SF scheme setup and investigate the property using the perturbation theory. The MDWFs we investigated include the optimal type domain wall, the overlap, the truncated domain wall, and the truncated overlap fermions. We observe the universality of the spectrum of the effective four-dimensional operator at the tree-level. The fermionic contribution to the universal one-loop beta function is reproduced for the MDWFs with a sufficiently large fifth dimensional extent.

*Keywords*: Lattice Field Theory; Lattice Chiral Symmetry; Renormalization

PACS numbers:11.15.Ha,11.10.Gh,11.30.Rd

## 1. Introduction

Chiral symmetry has played important roles in quantum field theories and in the low energy physics of Quantum Chromodynamics (QCD). Lattice field theory is a non-perturbative and first principle framework for quantum field theories and the lattice gauge theory has been successfully applied to describing the low energy properties of QCD.

A major disadvantage until mid-'90s in lattice QCD simulations was the lack of chiral symmetry on the lattice due to the Nielsen-Ninomiya's no-go theorem which implies the impossibility of constructing lattice fermions having chiral symmetry. Fortunately the situation has changed after the developments of the following lattice fermion theories; perfect action,[1,2] domain wall fermion,[3] and overlap fermion.[4–6] The notion of symmetry in these lattice fermions has been summarized in terms of the Ginsparg-Wilson relation[7] and the lattice chiral symmetry.[8] The overlap fermion exactly holds the lattice chiral symmetry, while the domain wall fermion approximately with a finite extent in the fifth-dimension. The lattice chiral symmetry is not the chiral symmetry, thereby a premise of the no-go theorem is circumvented.

The lattice chiral symmetry brings us benefit such as, no-fine tuning, no-operator mixing *etc.*, as existing in continuum field theories. The early review on the lattice chiral fermions can be seen in Refs. 9–11.

Although the simulation cost for the lattice chiral fermions is high, large scale simulations for lattice QCD employing the lattice chiral fermions have been being carried out supported by increasing computer performance in recent years.[12] The renormalization of lattice operators is required as usual and the non-perturbative renormalization scheme is preferable for the application to QCD and the Standard model calculations to reduce the systematic errors. The non-perturbative renormalization to the lattice chiral fermions is desired.

There exist several non-perturbative renormalization schemes applicable to lattice field theories; RI-MOM,[13,14] Schrödinger functional,[15–18] and Gradient-flow[19–24] *etc.* The Schrödinger functional (SF) scheme has been successfully applied for Wilson fermions to renormalize the lattice operators, coupling, and fermion masses, together with the $O(a)$-improvements.[15–18,25–35] The application of the SF scheme to the lattice chiral fermions is a natural path to extract the renormalization factors non-perturbatively. The SF scheme introduces a finite space-time box with a periodic boundary condition in the spatial directions and a Dirichlet boundary condition in the temporal direction. However the temporal boundary condition in the SF scheme contradicts the necessary conditions of the overlap and the domain wall fermions.[36,37] It was explicitly pointed out that the temporal boundary condition must violate the chiral symmetry and the Dirac fermion propagator has a non-trivial anti-commutation relation to $\gamma_5$ at the boundary in the continuum theory.[38] Therefore one must introduce an appropriate modification reflecting the boundary condition into the lattice chiral fermions so as to reproduce the same property as in the continuum limit. This means that the lattice chiral symmetry with the SF boundary condition becomes non-trivial.[36–38]

The SF scheme setup for the lattice chiral fermions is formulated in Refs. 36–41. Lüscher investigated chiral symmetry with the SF boundary condition in the continuum theory and pointed out a condition for the lattice chiral fermions to have the proper continuum limit based on universality arguments,[38] where the overlap fermion operator was modified so as to have proper continuum limit by explicitly violating the lattice chiral symmetry at the SF boundary. Subsequently the universality of the overlap fermion with the SF boundary condition was investigated perturbatively by Takeda.[40] According to the universality argument of Ref. 38, Takeda introduced a boundary term for the domain wall fermion to formulate the SF scheme and investigated the property perturbatively.[41]

In this paper we extend the work done by Takeda[41] to the Möbius domain wall fermions.[42,43] The Möbius domain wall fermion (MDWF) is a generalization of the domain wall fermion involving the truncated overlap fermion, optimal domain wall fermion, and overlap fermion as the limiting cases. One motivation of employing the MDWF is the reduction of the simulation cost with a better approximate lattice chiral symmetry. After tuning the parameters contained in the MDWF action, the

MDWF requires a smaller extent in the fifth direction compared to the standard domain wall fermion (SDWF) at the same approximate lattice chiral symmetry. When the parameters contained in the MDWF action are chosen to optimally, which corresponds to the optimal domain wall fermion, the lattice chiral symmetry can be realized numerically. The MDWF, therefore, enables us doing simulations at a cost effective manner with an approximate lattice chiral symmetry under controlled.[43,44] By developing the SF scheme for the MDWF we can cover a class of lattice chiral fermions applicable to the SF scheme. We thus aim at the non-perturbative renormalization with the SF scheme compatible both with a better control of the lattice chiral symmetry and with a low computational cost.

In order to find the boundary operator for the MDWF, we have to identify the boundary term that properly breaks the chiral symmetry at the temporal boundary in the SF scheme. The boundary operator should hold the discrete space-time symmetries: $C, P, T$, $\Gamma_5$-Hermiticity, but it must break the lattice chiral symmetry at the temporal boundary only. During this construction, we observe that the parameters of the MDWF, which depend on the fifth-index, must have parity symmetry in the fifth direction so as to hold the discrete symmetry. In this paper, we investigate the validity of the MDWF with the boundary term we constructed by observing the continuum limit of the effective four dimensional operator at the tree-level and the one-loop beta function perturbatively. Preliminary results of this work have been reported in Refs. 45, 46.

The paper is organized as follows. In section 2, we briefly introduce the SF formalism and the boundary condition. We give the property of the Dirac propagator under the chiral symmetry with the SF boundary condition.[38] Before proceeding to the construction of MDWF with the SF boundary, we clarify the property of the MDWF in the periodic boundary condition in section 3. The continuum limit of the effective four-dimensional operator[47] is also examined to identify the normalization and the residual mass[48] at the tree-level. Section 4 describes the construction of the MDWF operator with the temporal boundary term in the SF. In section 5 we numerically verify the continuum limit of the effective four dimensional operator of the MDWF with the SF boundary at the tree-level. In the preliminary work[46] we did not subtract the residual mass at the tree-level resulting a non-universal behavior at a small extra dimension size. We find that the residual mass must be subtracted to get at the correct continuum limit even at the tree-level. In section 6, we verify the fermionic part of the universal one-loop beta function. We conclude the paper in the last section 7.

## 2. Schrödinger Functional Scheme and Chiral Symmetry

In the Schrödinger Functional (SF) scheme,[15–18] the temporal and spatial extents are finite with the length $T$ and $L$ respectively. The Dirichlet boundary condition is imposed in the temporal direction so as to be consistent with the time evolution of the quantum system. The temporal coordinate $x_0$ is in $[0, T]$ and the spatial one

is $x_j \in [0, L]$. In order to concentrate on the property of the fermionic fields, we do not explain the details of the property of the gauge fields in the SF scheme in this paper.

We begin with the description on the fermionic fields in the continuum theory. The fermion field $\psi(x)$ in the SF scheme has the following boundary conditions.

$$P_+\psi(x)|_{x_0=0} = 0, \quad P_-\psi(x)|_{x_0=T} = 0, \tag{1}$$
$$\bar{\psi}(x)P_-|_{x_0=0} = 0, \quad \bar{\psi}(x)P_+|_{x_0=T} = 0, \tag{2}$$

with $P_\pm = (1 \pm \gamma_4)/2$. We employ the generalized boundary condition in the spatial direction,

$$\psi(x_0, \boldsymbol{x} + L\hat{j}) = e^{i\theta_j}\psi(x_0, \boldsymbol{x}), \tag{3}$$

where $\hat{j}$ is a unit vector in the $j$-th direction, and $\theta_j (j = 1, 2, 3)$ is a real parameter.

Although the mass-less Dirac propagator with the temporal boundary conditions Eq. (2) anti-commutes with $\gamma_5$

$$D\gamma_5 + \gamma_5 D = 0, \tag{4}$$

the mass-less Dirac propagator $S(x, y)$ does not anti-commute with $\gamma_5$ as

$$\gamma_5 S(x, y) + S(x, y)\gamma_5 = \int_{z_0=0} d\boldsymbol{z} S(x, z)\gamma_5 P_- S(z, y) + \int_{z_0=T} d\boldsymbol{z} S(x, z)\gamma_5 P_+ S(z, y). \tag{5}$$

This relation implies that the naive chiral symmetry does not hold in the SF scheme.[38]

On the lattice, the same SF boundary condition will be imposed on the lattice fermionic fields. The form of the Dirac propagator on the lattice depends on the choice of the lattice Dirac fermion action. One required condition for the lattice action is that the lattice Dirac propagator should satisfy Eq. (5) in the continuum limit. For the lattice chiral fermions the modification of the lattice action to satisfy the SF boundary condition is required.[36–38,41]

## 3. Properties of Möbius domain wall fermions in periodic boundary condition

Before introducing the SF scheme into the Möbius domain wall fermions (MDWF), we briefly explain the properties of the MDWF without the SF boundary condition. The temporal and spatial extent of the lattice box is infinite or finite with periodic boundary conditions for simplicity.

The MDWF operator[42,43] $D_{\rm MDWF}$ is defined by

$$D_{\rm MDWF} = \begin{pmatrix} D_1^{(+)} & D_1^{(-)}P_L & 0 & 0 & 0 & -m_f D_1^{(-)}P_R \\ D_2^{(-)}P_R & D_2^{(+)} & D_2^{(-)}P_L & 0 & 0 & 0 \\ 0 & D_3^{(-)}P_R & D_3^{(+)} & D_3^{(-)}P_L & 0 & 0 \\ 0 & 0 & D_4^{(-)}P_R & D_4^{(+)} & D_4^{(-)}P_L & 0 \\ 0 & 0 & 0 & D_5^{(-)}P_R & D_5^{(+)} & D_5^{(-)}P_L \\ -m_f D_6^{(-)}P_L & 0 & 0 & 0 & D_6^{(-)}P_R & D_6^{(+)} \end{pmatrix}, \quad (6)$$

$$D_j^{(+)} = D_W b_j + 1, \quad D_j^{(-)} = D_W c_j - 1, \quad (j = 1, 2, \cdots, N_5), \quad (7)$$

where $P_{L/R} = (1 \mp \gamma_5)/2$, $D_W$ is the four-dimensional Wilson-Dirac operator with a negative mass $m_0$ which corresponds to the domain wall height, and $m_f$ is the fermion mass. The size in the fifth-direction $N_5$ is assumed to be an even number and we use $N_5 = 6$ to explicitly display the operator in the five-dimensional form throughout this paper. The coefficients $b_j$ and $c_j$ are tunable parameters of the MDWF. They are chosen to optimize the lattice chiral symmetry with a minimum computational cost at a finite $N_5$. In this paper we usually use $a = 1$ for the lattice spacing "$a$" while we write $a$ explicitly when we deal with the continuum limit.

The effective four-dimensional operator, $D_{\rm eff}^{(N_5)}$, derived from the MDWF operator (6) is given by

$$D_{\rm eff}^{(N_5)} \equiv \epsilon^T P^T \left(D_{\rm PV}^{(N_5)}\right)^{-1} D_{\rm MDWF}^{(N_5)} P \epsilon, \quad (8)$$

where $D_{\rm PV}^{(N_5)}$ is defined by $D_{\rm PV}^{(N_5)} = D_{\rm MDWF}^{(N_5)}|_{m_f=1}$ coming from the Pauli-Villars fields eliminating the massive modes except the lightest one from the spectrum. The permutation and chiral projection matrix $P$, and the restriction vector $\epsilon$ are defined by

$$P = \begin{pmatrix} P_L & P_R & 0 & 0 & 0 & 0 \\ 0 & P_L & P_R & 0 & 0 & 0 \\ 0 & 0 & P_L & P_R & 0 & 0 \\ 0 & 0 & 0 & P_L & P_R & 0 \\ 0 & 0 & 0 & 0 & P_L & P_R \\ P_R & 0 & 0 & 0 & 0 & P_L \end{pmatrix}, \quad \epsilon = (1, 0, 0, 0, 0, 0)^T. \quad (9)$$

With periodic or infinite volume case, we can obtain the explicit form for the four-dimensional operator;[42,43,49–52]

$$D_{\rm eff}^{(N_5)} = \frac{1 + m_f}{2} + \frac{1 - m_f}{2} \gamma_5 R_{N_5}(\mathcal{H}_W). \quad (10)$$

The matrix function $R_{N_5}(x)$ in Eq. (10) is the rational approximation to the signum function

$$R_{N_5}(x) = \frac{\prod_{j=1}^{N_5}(1 + w_j x) - \prod_{j=1}^{N_5}(1 - w_j x)}{\prod_{j=1}^{N_5}(1 + w_j x) + \prod_{j=1}^{N_5}(1 - w_j x)}. \quad (11)$$

The matrix $\mathcal{H}_W$ in the argument is

$$\mathcal{H}_W = \gamma_5 D_W (a_5 D_W + 2)^{-1}. \tag{12}$$

The coefficients $(w_j, a_5)$ and the MDWF parameters $(b_j, c_j)$ have the following relation;

$$b_j + c_j = w_j, \quad b_j - c_j = a_5. \tag{13}$$

This is one of the parameter choice as the normalization of $\mathcal{H}_W$ can be absorbed in the definition of $w_j$. To be specific we employ the following parameterization for the Shamir kernel and the overlap kernel;

$$\mathcal{H}_W = \gamma_5 D_W (D_W + 2)^{-1}, \quad \text{with } b_j + c_j = w_j, b_j - c_j = 1, \tag{14}$$

for the Shamir kernel, and

$$\mathcal{H}_W = \gamma_5 D_W, \quad \text{with } b_j = c_j = w_j, \tag{15}$$

for the overlap kernel. We investigate these two kernels throughout the paper.

The effective four-dimensional operator Eq. (10) reduces to the overlap operator in the limit of $N_5 \to \infty$ provided by the convergence of the approximation to the signum function with a given $(b_j, c_j)$. The MDWF operator generalizes the domain wall type fermion operators including the standard domain wall, Boriçi's domain wall,[49–51] and optimal Chiu's domain wall[52] fermions. The overlap operator, $D_{\rm OVF}$, in the limiting case satisfies the Ginsparg-Wilson (GW) relation,[7]

$$\gamma_5 D_{\rm OVF} + D_{\rm OVF}\gamma_5 = \frac{2}{1+m_f}\left(m_f\gamma_5 + D_{\rm OVF}\gamma_5 D_{\rm OVF}\right). \tag{16}$$

At a finite $N_5$ the effective four-dimensional operator $D_{\rm eff}^{(N_5)}$ does not satisfy the GW relation due to the explicit breaking of the lattice chiral symmetry. In order to investigate the chiral property in the SF scheme at a finite $N_5$, the explicit breaking must be taken into account. Taking the continuum limit of Eq. (10) at the tree-level, we obtain

$$aD_{\rm eff}^{(N_5)} \to Z\left[ia\not{\partial} + am_{\rm res}\right], \tag{17}$$

$$Z = \frac{(1-am_f)R_{N_5}(\alpha)}{(am_0)(2-(am_0)a_5)}, \tag{18}$$

$$am_{\rm res} = \left[\frac{1+am_f}{1-am_f}\frac{1}{R_{N_5}(\alpha)} - 1\right]\frac{(am_0)(2-(am_0)a_5)}{2}, \tag{19}$$

$$\alpha = \frac{(am_0)}{2-(am_0)a_5}. \tag{20}$$

There is a residual mass $am_{\rm res}$ in $D_{\rm eff}^{(N_5)}$ even at the tree-level with $m_f = 0$.[48] The residual mass vanishes in $N_5 \to \infty$ as $R_{N_5}(\alpha) \to 1$.

The analysis in this section is based on the explicit form of the effective four-dimensional operator Eq. (10). In the next section we introduce a MDWF operator for the SF scheme by modifying Eq. (6). We use the normalization $Z$ of Eq. (18)

and the residual mass $am_{\rm res}$ of Eq. (19) for the modified MDWF operator with the SF boundary condition, despite $Z$ and $am_{\rm res}$ are obtained in the periodic boundary condition.

## 4. Möbius domain wall fermions with the Schrödinger functional boundary condition

The SF scheme is defined in a finite four-dimensional box. The lattice extent in the spatial direction is $N_S = L/a$ and the temporal one is $N_T = T/a$. The lattice index in the spatial direction $n_k, k = 1, 2, 3$ runs in $0, 1, \cdots, N_S - 1$, while the temporal index $n_4$ runs in $1, 2, \cdots, N_T - 1$. The fields at $n_4 = 0$ and $n_4 = N_T$ are fixed by the Dirichlet boundary conditions (2).

According to the universality argument given by Lüscher[38] and the realization of the SF scheme for the standard domain wall fermion by Takeda,[41] we modify the MDWF operator Eq. (6) by adding a boundary operator $B_{\rm SF}$ as follows.

$$D^{\rm SF}_{\rm MDWF} = D_{\rm MDWF} + c_{\rm SF} B_{\rm SF}, \tag{21}$$

$$B_{\rm SF} = \begin{pmatrix} 0 & 0 & 0 & 0 & 0 & -D_1^{(-)}B \\ 0 & 0 & 0 & 0 & -D_2^{(-)}B & 0 \\ 0 & 0 & 0 & -D_3^{(-)}B & 0 & 0 \\ 0 & 0 & D_3^{(-)}B & 0 & 0 & 0 \\ 0 & D_2^{(-)}B & 0 & 0 & 0 & 0 \\ D_1^{(-)}B & 0 & 0 & 0 & 0 & 0 \end{pmatrix}. \tag{22}$$

The boundary operator $B$ is defined by

$$B(n, m) = \delta_{n,m}\gamma_5(\delta_{n_4,1}P_L + \delta_{n_4,N_T-1}P_R). \tag{23}$$

The temporal hopping terms from $n_4 = 0$ and $n_4 = N_T$ in the Wilson-Dirac operator contained in Eq. (21) are set to be zero as the SF boundary condition.

$B_{\rm SF}$ has supports only at $n_4 = 1$ and $N_T - 1$, and explicitly violates the domain wall chiral symmetry[53] at $n_4 = 1$ and $N_T - 1$. We expect that the lattice chiral symmetry is still maintained in the bulk region. The coefficient $c_{\rm SF}$ is a non-zero parameter to remove the $O(a)$-discretization error from the boundary effect. Although the form of $B_{\rm SF}$ is a naive extension of Takeda's realization, we need the parity symmetry in the fifth-direction in order to keep the discrete symmetries, $C, P, T$ and $\Gamma_5$-Hermiticity. This parity symmetry is not required in the periodic boundary or infinite extent cases. Nevertheless it seems to have theoretical benefits to analyze the operator and the action.[42,53–56]

The effective four-dimensional operator for Eq. (21) is defined by Eq. (8). We, however, could not extract a simple short form for the effective four-dimensional operator similar to Eq. (10). The ordering of $b_j$ and $c_j$ is irrelevant as seen in Eq. (10) in the periodic or infinite volume cases, while it affects the form of the effective four-dimensional operator in the SF scheme, *i.e.* a different choice for the ordering

yields a different effective operator. This ordering dependence must disappear in the continuum limit as the SF scheme is regularization independent.

At a finite $N_5$ the degree of freedom for $b_j$ and $c_j$ to optimize the lattice chiral symmetry with the SF boundary is halved from that without the SF boundary due to the parity symmetry constraint. Therefore we cannot not use the optimal choice for the coefficients $b_j$ and $c_j$ such as given by Chiu.[52] A choice for the coefficients has been given in Refs. 54, 55. Optimal coefficients with the parity constraint has been formulated in Ref. 57. Instead of the optimal coefficients of Ref. 57, we employ a quasi optimal coefficients in which we duplicate the half order $(N_5/2)$ coefficients from the Zolotarev optimal coefficients[52,58] to make $N_5$ coefficients. The property of the quasi optimal choice has been surveyed in our previous study[46] and we checked that the discrepancy between the quasi optimal and optimal[57] was small for $N_5 \gtrsim 10$.

Although we cannot extract the rational approximation $R_{N_5}(x)$ with the boundary term $B_{\rm SF}$, we assume that the same rational form is valid in the bulk region because the boundary effect becomes small as we extend the temporal extent. We use the same form for the normalization $Z$ and the residual mass $am_{\rm res}$ with the SF boundary for the same reason. The choice of the coefficients $b_j$ and $c_j$ is still important to maintain the lattice chiral symmetry in the bulk region. To determine $b_j$ and $c_j$ from the approximation range for the signum function we use the spectrum of the kernel operator Eq. (12) with the Wilson-Dirac fermion operator $D_W$ satisfying the SF boundary condition.

## 5. Tree-Level Analysis of Möbius Domain Wall Fermions with the SF boundary condition

We investigate the properties of the effective four-dimensional operator built with the MDWF with the SF boundary term Eq. (21) at the tree-level. The spectrum, the temporal structure of the GW relation, and the propagator will be investigated at the tree-level in this section. After checking the universality to the continuum limit, we will examine the fermionic contribution to the one-loop beta function in the next section.

The classical background field induced by the SF boundary gauge field must be incorporated in the analysis for the one-loop beta function. The classical background gauge field is given by

$$U_k(n) = \exp\left[i\frac{1}{N_T}\left(n_4\phi'_k + (N_T - n_4)\phi_k\right)\right], \quad U_4(n) = 1. \tag{24}$$

This is induced by the boundary field

$$U_k(n)|_{n_4=0} = e^{i\phi_k}, \quad U_k(n)|_{n_4=N_T} = e^{i\phi'_k}, \tag{25}$$

for the spatial gauge fields $(k = 1, 2, 3)$ at $n_4 = 0$ and $N_T$. $\phi_k$ and $\phi'_k$ are color-

diagonal matrices defined by

$$\begin{aligned}\phi_k &= \frac{1}{N_S}\mathrm{diag}\left(\eta\omega_1 - \frac{\pi}{3}, \eta\omega_2, \eta\omega_3 + \frac{\pi}{3}\right),\\ \phi'_k &= \frac{1}{N_S}\mathrm{diag}\left(-\eta\omega_1 - \pi, -\eta\omega_3 + \frac{\pi}{3}, -\eta\omega_2 + \frac{2\pi}{3}\right),\\ (\omega_1, \omega_2, \omega_3) &= (1, -1/2, -1/2).\end{aligned} \tag{26}$$

The effective four-dimensional operator is renormalized using Eqs. (18) and (19) as

$$D_q = Z^{-1} D_{\mathrm{eff}}^{(N_5)}. \tag{27}$$

We investigate the spectrum, the chiral property in the GW relation, and the propagator of the renormalized $D_q$ with and without the background field in the following.

### 5.1. *Spectrum of the effective four-dimensional operator*

We investigate the spectrum of the Hermitian squared effective four-dimensional operator $D_q^\dagger D_q$ in boxes with $N_T = N_S$ with and without the nonzero background field. We show $b_j = c_j = w_j$ cases which correspond to the overlap fermion in the $N_5 \to \infty$ limit. This choice is a nontrivial check to the standard domain wall fermion because $c_j \neq 0$ is the new structure for the MDWF.

The quasi optimal values for the MDWF parameters $(b_j, c_j)$ are determined by specifying the approximation range and the order $N_5/2$ of the Zolotarev approximation formula. We use the spectrum of the kernel operator Eq. (12) to determine the approximation range. We investigate the lowest and highest eigenvalues of the kernel operator with the SF background field and $\theta = \pi/5$. We obtain

$$0.361893\frac{1}{N_S} < a|\mathcal{H}_W| < 1.0, \tag{28}$$

for the Shamir kernel Eq. (14), and

$$0.725254\frac{1}{N_S} < a|\mathcal{H}_W| < 7.0, \tag{29}$$

for the overlap kernel Eq. (15) from the asymptotic behavior to the continuum limit. The lowest eigenvalue approaches to zero as we take the continuum limit with fixing $L = aN_S$ at a constant. This means that the approximation to the signum function becomes worse with a fixed $(b_j, c_j)$ when the lower spectrum spills over the approximation range in taking the continuum limit.

The MDWF parameters $b_j$ and $c_j$ used in the spectrum test are listed in Table 1, which is obtained from the $N_5 = 4$ optimal Zolotarev approximation coefficient. The signum function approximation range and the accuracy of the original coefficients $w_j (j = 1, \cdots, 4)$ are $x \in [0.01, 7.00]$ and $|1 - R_4(x)| \lesssim 0.324$ respectively. This approximation is valid with $N_S < 72$ as seen from Eq. (29) in the cases with the SF background field and $\theta = \pi/5$. The signum function with the parity symmetric

Table 1. The MDWF parameters $b_j(= c_j)$. The signum function approx-imation parameters are $w_j = b_j$.

| $j$ | $b_j$ |
|---|---|
| $1, 8$ | 0.237921110807 |
| $2, 7$ | 1.265028710883 |
| $3, 6$ | 11.29279846601 |
| $4, 5$ | 60.04391219119 |

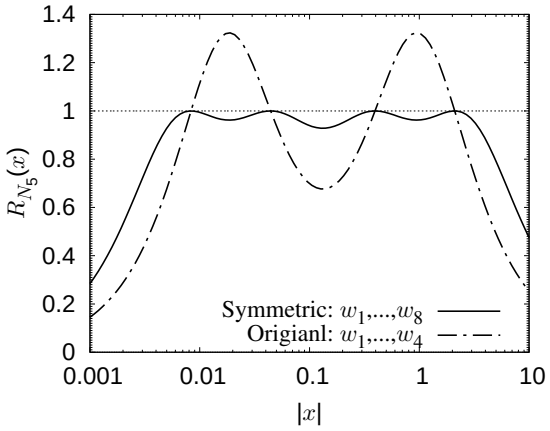


Fig. 1. The signum function approximation with Eq. (11). "Original" uses $w_1, \cdots, w_4$ which corresponds to the fourth order optimal Zolotarev approximation, while "Symmetric" uses all coefficients from Table 1.

coefficients in the fifth-direction, $w_j (j = 1, \cdots, 8)$, has the accuracy of $|1 - R_8(x)| \lesssim 0.072$ (Fig. 1).

The lowest ten eigenvalues at $am_{\rm res} = 0$ are shown in Figure 2 as a function of $a/L = 1/N_S$. The boundary coefficient is $c_{\rm SF} = 1$. The solid circles at $a/L = 0$ (continuum limit) are computed with a variational method in the continuum theory.[16] We use $Z = 0.99659683271$ for the normalization Eq. (18) and $am_{\rm cr} = -0.0034031673$ where $am_{\rm res}|_{am_f = am_{\rm cr}} = 0$ from Eq. (19).

The spectrum properly converges to the continuum limit even at a smaller $N_5 = 8$, which supports the use of the normalization (18) and residual mass subtraction (19) even with the SF boundary condition. We confirm the same behavior for other parameters: a larger $N_5$, $am_{\rm res} \neq 0$, a reverse order of $b_j$, and other overlap kernels $(b_j + c_j = 1)$ and $(b_j = 1, c_j = 1)$.

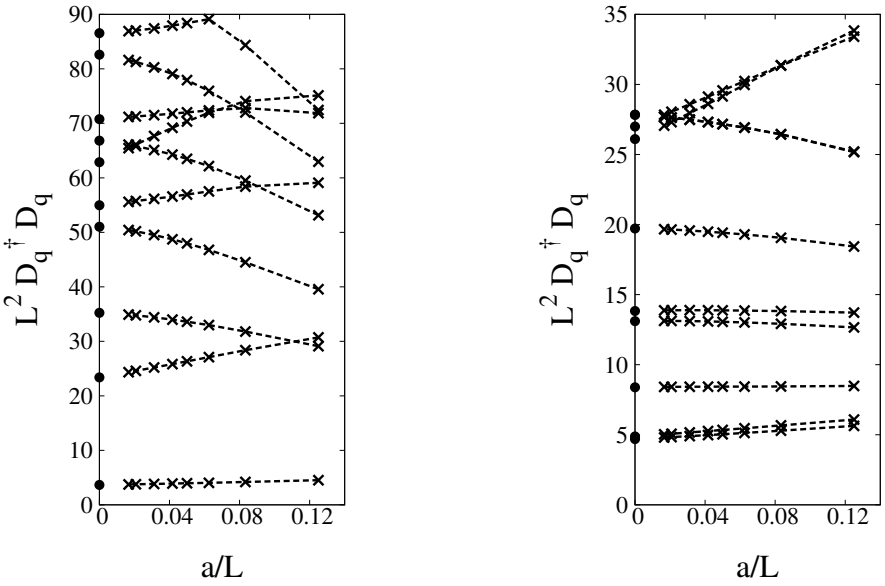


(a) Without the background field ($\phi_k = \phi'_k = 0$).

(b) With the background field ($\phi_k|_{\eta=0}, \phi'_k|_{\eta=0}$).

Fig. 2. The lowest ten eigenvalues of the MDWF with $c_j = b_j = w_j$, $N_5 = 8$, $am_{\rm res} = 0$, $\theta = \pi/5$ and $c_{\rm SF} = 1$. $w_j$ are taken from the optimal Zolotarev approximation with the approximation range $x \in [0.01; 7.00]$ at the given order.

### 5.2. *Dirac propagator from the effective four-dimensional operator*

The GW relation for the effective operator $D_q(n, m)$ in the temporal direction is investigated at the vanishing spatial momentum and mass. The GW relation violation is measured with

$$\delta(n_4, m_4) = \sum_{\rm color,spin} \left| \{\gamma_5, \tilde{D}_q(n_4, m_4)\} - 2\tilde{D}_q(n_4, m_4)\gamma_5 \tilde{D}_q(n_4, m_4) \right|, \qquad (30)$$

where $\tilde{D}_q(n_4, m_4)$ is the zero-momentum part of $D_q(n, m)$.

Figure 3 shows the GW relation violation with the background field and $\theta = \pi/5$. The boundary coefficient is $c_{\rm SF} = 1$. The operator is $c_j = b_j = w_j$ using the quasi optimal approximation. The approximation range is fixed to $x \in [0.01, 7.00]$ for all $N_5$. The gray scale corresponds to $\log_{10}(\delta(n_4, m_4))$. As we increase $N_5$ the violation in the bulk temporal region vanishes, while it remains at the temporal boundary as we expected. The same behavior is observed for other kernel operators with different parameters.

The Dirac propagator with the SF boundary condition in vanishing background field is analytically given in the continuum theory,[16] to which we can compare directly the lattice Dirac propagator. Figs 4 and 5 show the time dependence of the

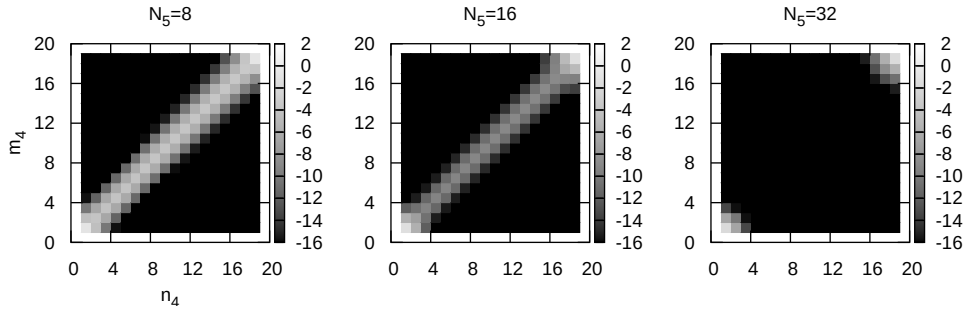


Fig. 3. The GW relation violation (30) of the MDWF with $c_j = b_j = w_j$ and $c_{\rm SF} = 1$. $w_j$ are taken from the optimal Zolotarev approximation with the approximation range $x \in [0.01, 7.00]$ at the given order. The background field exists.

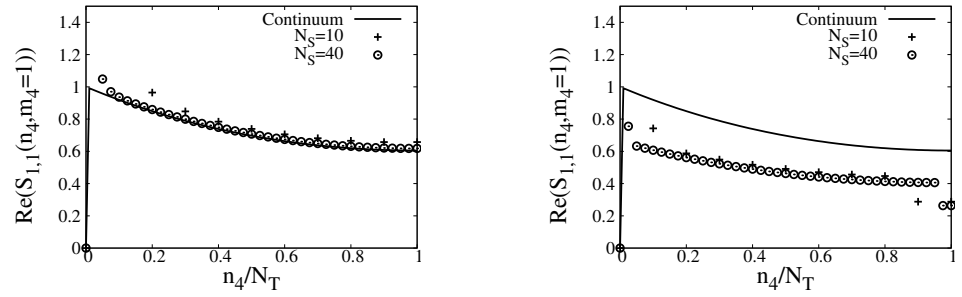


(a) The Standard Shamir DWF (b) The Boriçi DWF

Fig. 4. The real part of the spin $(1,1)$-component of the Dirac propagator from $m_4 = 1$. Zero background field, $am_{res} = 0$, $\theta = 0$, and $N_5 = 16$.

real part of the spin $(1,1)$ component of the Dirac propagator. We use the Dirac representation for the $\gamma$-matrices. The boundary coefficient is $c_{\rm SF} = 1$. The source time $m_4$ is $m_4 = 1$ in Fig. 4 and $m_4 = 2$ in Fig. 5 respectively. The solid line represents the analytic solution in the continuum theory. The cut-off dependence of the lattice propagator can be compared at $L/a = N_S = 10$ (crosses) and $L/a = N_S = 40$ (open circles).

From the left panel (4(a)), we see that the propagator with the standard domain wall fermion $(b_j = 1, c_j = 0)$ converges to the continuum limit properly. On the other hand, in the right panel (4(b)), the propagator with the Boriçi domain wall fermion $(b_j = 1, c_j = 1)$[49–51] does not converge to the continuum line. To check the boundary effect further we plot the Dirac propagator propagating from $m_4 = 2$ in Figure 5. The left panel (5(a)) shows the standard domain wall fermion and is consistent with the continuum limit. The Boriçi domain wall fermion in the right panel (5(b)) is now consistent with the continuum limit. We observe the same behavior for other non-zero spin components that touching the surface time slices $n_4 = 1$ or $n_4 = N_T - 1$

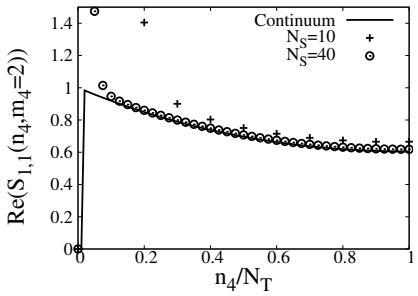


(a) The Standard Shamir DWF

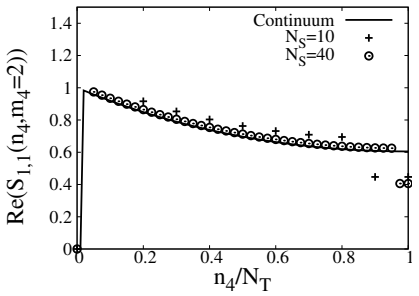


(b) The Boriçi DWF

Fig. 5. The same as Fig. 4, but propagates from $m_4 = 2$.

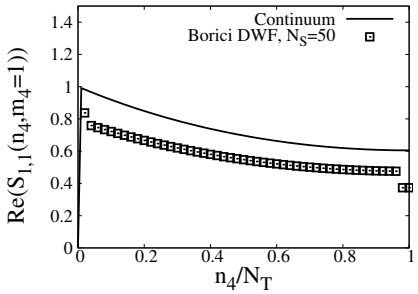


(a) The Boriçi DWF.

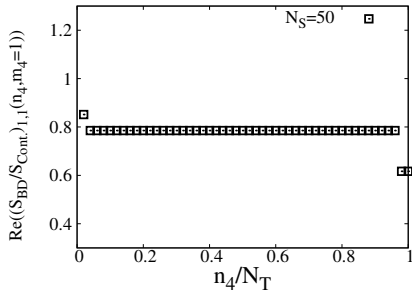


(b) The time dependence of the ratio of the Boriçi DWF to the continuum

Fig. 6. The real part of the spin $(1,1)$-component of the Dirac propagator from $m_4 = 1$. The Boriçi DWF with $c_{\rm SF} = 0.4167$, Zero background field, $am_{res} = 0$, $\theta = 0$, and $N_5 = 16$ is shown.

(interior time surfaces of the SF boundary condition). This behavior is common to other MDWFs with $c_j \neq 0$. Thus the boundary effect at the tree-level exists for the MDWFs with $c_j \neq 0$. The boundary coefficient $c_{\rm SF}$ can be tuned to eliminate the boundary $O(a)$ error, however the discrepancy does not proportional to $a$ as seen in Figure 4(b) and cannot be removed by tuning $c_{\rm SF}$.

In order to see the property of the discrepancy further, we investigate the ratio of the propagator of the Boriçi domain wall fermion to that of the continuum theory. Figure 6 shows the real part of the spin $(1,1)$-component of the propagator with the Boriçi DWF with the tuned $c_{\rm SF}$ parameter, $c_{\rm SF} = 0.4167$, which is determined by the PCAC relation to be described in the next subsection. The discrepancy still remains (Fig. 6(a)) even with the tuned $c_{\rm SF}$. Figure 6(b) shows the time dependence of the ratio. The discrepancy is constant in time. We observe that the constant value is common to the other spin components and other source time $m_4 = N_T - 1$.

We found that this inconsistency of the propagator touching the surface time

slices at $n_4 = 1$ or $n_4 = N_T - 1$ are common to other MDWFs with $c_j \neq 0$. The propagator we showed so far is without the background field. With the SF background field, the same behavior is observed for the MDWFs with $c_j \neq 0$. A constant factor discrepancy in the continuum limit remains in the propagator touching the surface time slices at $n_4 = 1$ or $n_4 = N_T - 1$. This strongly suggests the boundary effect introduced by Eq. (22).

From these observations, we need a constant renormalization to the propagator touching the surface time slices. We have a degree of freedom to renormalize the boundary operator of the fermion fields.[16,18] The boundary operator places at $n_4 = 0$ and $n_4 = N_T$ in the SF scheme can be renormalized independently from the bulk fermion fields. A subtlety arises for the renormalization on the (effective four dimensional) fermion fields on the surface time slices at $n_4 = 1$ and $n_4 = N_T - 1$. We could not find any counter term for the fermion fields on $n_4 = 1$ and $n_4 = N_T - 1$, and any analytic representation for the renormalization factor. We expect this renormalization can be absorbed into the boundary operator renormalization as the distinction between the boundary and the interior surface disappear eventually in the continuum limit.

### 5.3. *Tuning on the boundary coefficient* $c_{\rm SF}$

The boundary operator Eq. (22) causes an $O(a)$ error in the bulk spectrum. According to Refs. 38, 40, 41, we employ the PCAC relation to remove the $O(a)$ error by tuning the boundary coefficient $c_{\rm SF}$.

In the continuum the two-point correlation functions used for the PCAC relation are defined by

$$f_A(x_4) = -\frac{1}{(N_f^3-1)L^3}\int d^3\boldsymbol{x} d^3\boldsymbol{y} d^3\boldsymbol{z} \langle A_4^a(x) O^a(\boldsymbol{y},\boldsymbol{z})\rangle, \tag{31}$$

$$f_P(x_4) = -\frac{1}{(N_f^3-1)L^3}\int d^3\boldsymbol{x} d^3\boldsymbol{y} d^3\boldsymbol{z} \langle P^a(x) O^a(\boldsymbol{y},\boldsymbol{z})\rangle, \tag{32}$$

$$A_\mu^a(x) = \bar\psi(x)\gamma_\mu\gamma_5 T^a\psi(x), \quad P^a(x) = \bar\psi(x)\gamma_5 T^a\psi(x),$$
$$O^a(\boldsymbol{y},\boldsymbol{z}) = \bar\psi(y)\gamma_5 T^a\psi(z)|_{y_4=z_4=0}, \tag{33}$$

with the generators $T^a$ of SU($N_f$) flavor symmetry. The two-point functions with vanishing background field in the continuum theory at the tree-level become

$$f_A(x_4) = -\frac{N_c}{R^2}\left[E^2 - m^2 + m\{m\cosh(2E(T-x_4)) + E\sinh(2E(T-x_4))\}\right], \tag{34}$$

$$f_P(x_4) = \frac{N_c E}{R^2}\left[E\cosh(2E(T-x_4)) + m\sinh(2E(T-x_4))\right], \tag{35}$$

$$R = E\cosh(ET) + m\sinh(ET), \quad E = \sqrt{\boldsymbol{p}_0^2 + m^2}, \quad \boldsymbol{p}_0 = \theta/L, \tag{36}$$

where $N_c$ is the number of color. The ratio at $x_4 = T/2$ and $T = 2L$ with $m = 0$

Table 2. Optimal values for $c_{\rm SF}$.

| $b_j, c_j$ | $b_j = 1, c_j = 0$ | $b_j = c_j = 1$ | $b_j + c_j = w_j, b_j - c_j = 1$ | | | $b_j = c_j = w_j$ | | |
|---|---|---|---|---|---|---|---|---|
| $m_0$ | 1.5 | 1.5 | 1.0 | | | 1.0 | | |
| $N_5$ | 32 | 32 | 8 | 16 | 32 | 8 | 16 | 32 |
| $c_{\rm SF}$ | 0.520 | 0.312 | 0.820 | 0.630 | 0.5432 | 0.553 | 0.392 | 0.256 |

becomes

$$\frac{f_A(T/2)}{f_P(T/2)} = -\frac{1}{\cosh(2\sqrt{3}\theta)}. \tag{37}$$

The two-point functions with $D_q$ on the lattice are given by

$$f_A(n_4) = \frac{-1}{2N_S^3}\mathrm{Tr}\left[\tilde{S}(n_4,1)^\dagger \gamma_4 \tilde{S}(n_4,1)\right], \tag{38}$$

$$f_P(n_4) = \frac{1}{2N_S^3}\mathrm{Tr}\left[\tilde{S}(n_4,1)^\dagger \tilde{S}(n_4,1)\right], \tag{39}$$

where $\tilde{S}(n_4, m_4)$ is the zero-momentum projection of $S(n,m) = (D_q)^{-1}(n,m)$.

The tuning on $c_{\rm SF}$ is carried out by fitting $f_A(T/2)/f_P(T/2)$ as a polynomial function of $c_{\rm SF}$ and $a/L$, and eliminating the $O(a/L)$ term by tuning $c_{\rm SF}$. The surface field renormalization is not required for the ratio as it cancels. We fit $f_A(T/2)/f_P(T/2)$ with

$$\begin{aligned} f_A(T/2)/f_P(T/2) = A_{00} &+ (A_{01} + A_{11}c_{\rm SF} + A_{21}c_{\rm SF}^2 + A_{31}c_{\rm SF}^3)(a/L) \\ &+ (A_{02} + A_{12}c_{\rm SF} + A_{22}c_{\rm SF}^2 + A_{32}c_{\rm SF}^3)(a/L)^2 \\ &+ (A_{03} + A_{13}c_{\rm SF} + A_{23}c_{\rm SF}^2 + A_{33}c_{\rm SF}^3)(a/L)^3 + \cdots . \end{aligned} \tag{40}$$

$A_{00}$ can be fixed to its continuum value, for which Eq. (37) can be used when there is no background field. The optimal value of $c_{\rm SF}$ is thus obtained by solving

$$A_{01} + A_{11}c_{\rm SF} + A_{21}c_{\rm SF}^2 + A_{31}c_{\rm SF}^3 = 0. \tag{41}$$

Table 2 shows the tuning results for several types of the MDWF, where the tuning is done without the background field. The quasi optimal parameters used for $b_j + c_j = w_j, b_j - c_j = 1$ (Optimal Shamir) and $b_j = c_j = w_j$ (Optimal Chiu) are listed in Table A1 in Appendix A.

To see the effect of the tuning on $c_{\rm SF}$, we show the relative discrepancy of the ratio $f_A(n_4)/f_P(n_4)$ between the continuum theory and the lattice theory for the Boriçi domain wall fermion in Figure 7. The left figure (7(a)) is plotted with $c_{\rm SF} = 1$ and the right (7(b)) is with the tuned parameter $c_{\rm SF} = 0.312$. In both cases the discrepancy vanishes in the continuum limit ($N_S \to \infty$). This also shows that the surface field renormalization is just a constant and does not affect the bulk region. The rate of the convergence is faster for the tuned case (right figure). To see the convergence rate more explicitly, we plot the discrepancy at $t = T/2$ in Figure 8 as a function of $1/N_T^2 = (a/T)^2$. The convergence rate is $O(a^2)$ with the tuned coefficient (Fig. 8(b)). We also observed a similar behavior for other types of the

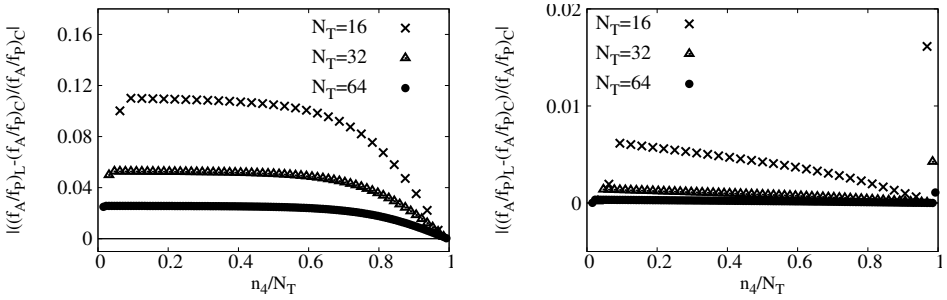


(a) $c_{\rm SF} = 1$. (b) $c_{\rm SF} = 0.312$.

Fig. 7. The time dependence of the discrepancy of $f_A(n_4)/f_P(n_4)$ between the continuum and the lattice theories. Boriçi domain wall fermion ($b_j = c_j = 1$) with $N_5 = 16$ is compared.

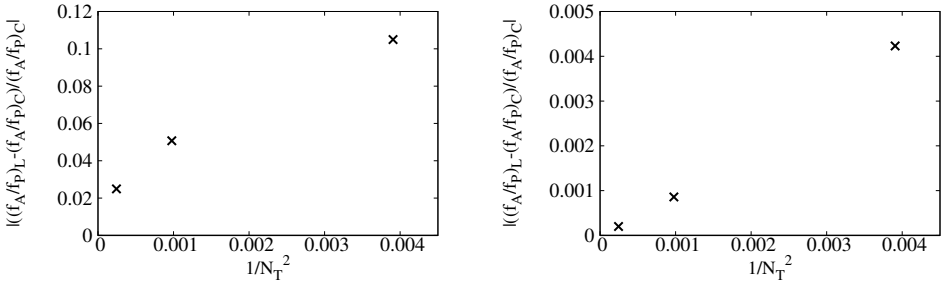


(a) $c_{SF} = 1$. (b) $c_{\rm SF} = 0.312$.

Fig. 8. $1/N_T^2$ dependence of the discrepancy of $f_A(N_T/2)/f_P(N_T/2)$ between the continuum and the lattice theories. Boriçi domain wall fermion ($b_j = c_j = 1$) with $N_5 = 16$ is compared.

MDWF including those with the quasi optimal coefficients for $(b_j, c_j)$ from the Zolotarev approximation.

From the observations we made in this section, we conclude that the MDWF with the SF boundary term Eq. (22) properly reproduces the continuum theory in the most bulk region by including the renormalization at the tree-level. However, with our implementation of the SF boundary setting for the MDWF, the interior surface field at the boundary needs a special renormalization at the tree-level, for which we did not find any appropriate counter term for the renormalization explicitly in the theory, though one possible counter term could come from the boundary field.

## 6. Fermionic contribution to the one-loop beta function

The renormalized coupling constant in the SF scheme $g_{\rm SF}$ is defined by

$$\frac{1}{g_{\rm SF}^2} = \frac{1}{k}\frac{\partial\Gamma}{\partial\eta}\bigg|_{\eta=0}, \tag{42}$$

$$\Gamma = -\log Z(\eta), \tag{43}$$

$$Z(\eta) = \int \mathcal{D}U\mathcal{D}\bar{\psi}\mathcal{D}\psi\Psi_f[U,\bar{\psi},\psi,\eta]^*\Psi_i[U,\bar{\psi},\psi,\eta]e^{-S_g[U]-S_q[U,\bar{psi},\psi]}, \tag{44}$$

where $Z(\eta)$ is the partition function, $\Psi_i$ and $\Psi_f$ are the initial ($n_4 = 0$) and final ($n_4 = N_T$) wave-functionals. The spatial gauge field at $n_4 = 0$ and $n_4 = N_T$ are fixed to Eq. (25) by the delta wave-functionals contained in $\Psi_i$ and $\Psi_f$. $\eta$ parametrizes the SF boundary condition as seen in Eqs. (25) and (26). $S_g$ is a lattice gauge action which has Eq. (24) as the classical solution, and $S_q$ is a fermion action. $k$ is a normalization constant depending on the gauge action $S_g$ and is determined so as to satisfy $g_{\rm SF} = g_0$ at the tree-level.

We employ the MDWF action for $S_q$ by introducing the five-dimensional fermion field $\Psi$ together with the Pauli-Villars field $\Phi$;

$$S_q = \bar{\Psi}D_{\rm MDWF}^{(N_5)}\Psi + \frac{1}{2}\Phi^* D_{\rm PV}^{(N_5)}\Phi. \tag{45}$$

Using the coupling expansion and the saddle-point approximation, the effective action $\Gamma$ is expanded as

$$\Gamma = \frac{1}{g_0^2}\Gamma^{(0)} + \Gamma^{(1)} + \cdots. \tag{46}$$

We focus on the fermionic contribution to $\Gamma^{(1)}$. The one-loop contribution to $g_{\rm SF}$ is parametrized as

$$g_{\rm SF}^2 = g_0^2 + p_1 g_0^4 + \cdots, \quad p_1 = p_{1,0} + N_f p_{1,1}, \tag{47}$$

where $N_f$ is the number of flavors which we include to tag the fermionic contribution $p_{1,1}$. $p_{1,1}$ can be evaluated via

$$p_{1,1} = \frac{1}{k}\sum_{\boldsymbol{p}} {\rm Tr}\left[\frac{\partial\tilde{D}_{\rm MDWF}^{(N_5)}}{\partial\eta}\left(\tilde{D}_{\rm MDWF}^{(N_5)}\right)^{-1} - \frac{\partial\tilde{D}_{\rm PV}^{(N_5)}}{\partial\eta}\left(\tilde{D}_{\rm PV}^{(N_5)}\right)^{-1}\right]\bigg|_{\eta=0}, \tag{48}$$

where the summation on $\boldsymbol{p}$ is done in the discrete momentum $\boldsymbol{p} = (2\pi\boldsymbol{n} + \theta)/N_S, n_k = 0, 1, \cdots, N_S - 1$. $\tilde{D}_{\rm MDWF}^{(N_5)}$ and $\tilde{D}_{\rm PV}^{(N_5)}$ are the spatial momentum projection of $D_{\rm MDWF}^{(N_5)}$ and $D_{\rm PV}^{(N_5)}$ respectively. The trace is over the color, spin, temporal lattice, and fifth-direction lattice indexes. The asymptotic form in $a \to 0$ is expected to be

$$p_{1,1} \sim \sum_{k=0}^{\infty}\left[r_k + s_k \ln(L/a)\right](a/L)^k, \tag{49}$$

where $s_0$ should coincide with the one-loop beta function $s_0 = 2b_{0,1} = -1/(12\pi^2) \simeq -0.00844343\cdots$.

Table 3. The parameter set used for $p_{1,1}$ in Eq. (48).

| $(b_j, c_j)$ | $m_0$ | $N_5$ | $m_{cr}$ | $c_{\rm SF}$ | lattice sizes $L/a$ |
|---|---|---|---|---|---|
| $(1,0)$ | 1.5 | 8 | $-0.0039062500$ | 0.520 | $[4:48]$ |
| | | 16 | $-0.0000152588$ | | $[4:48]$ |
| | | 32 | $-0.0000000002$ | | $[4:48]$ |
| $(1,1)$ | 1.0 | $8, 16, 32$ | 0.0 | 0.4167 | $[4:48]$ |
| | 1.5 | 8 | $-0.0000025600$ | 0.312 | $[4:80]$ |
| | | $16, 32$ | 0.0 | | $[4:48]$ |
| $b_j + c_j = w_j$ $b_j - c_j = 1$ | 1.0 | 8 | $-0.0475081142$ | 0.820 | $[4:80]$ |
| | | 16 | $-0.0003037107$ | 0.630 | $[4:48]$ |
| | | 32 | $-0.0000000216$ | 0.5432 | $[4:48]$ |
| $(w_j, w_j)$ | 1.0 | 8 | $-0.0034031673$ | 0.553 | $[4:72]$ |
| | | 16 | $-0.0000393319$ | 0.392 | $[4:72]$ |
| | | 32 | $-0.0000000029$ | 0.256 | $[4:48]$ |

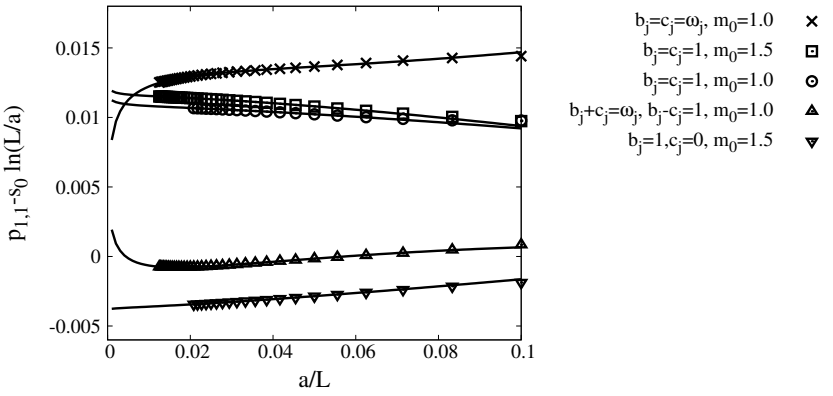


Fig. 9. $p_{1,1} - s_0 \ln(L/a)$ as a function of $a/L$ with $N_5 = 8$. The solid lines are the fit results using the data $a/L < 0.05$.

We numerically evaluate Eq. (48) with $N_S = N_T$ using the parameters shown in Table 3 by varying the lattice sizes in steps of 2 in the given range. For the optimal type domain wall fermions, we use the quasi optimal coefficients $(b_j, c_j)$ shown in Table A1 in Appendix A. The approximation range is fixed to $x \in [0.001 : 1.00]$ for the optimal Shamir domain wall fermion $(b_j + c_j = w_j, b_j - c_j = 1)$, and $x \in [0.01 : 7.00]$ for the optimal Chiu domain wall fermion $(b_j = c_j = w_j)$. The largest lattice sizes for the optimal type MDWF's satisfy the approximation boundary condition Eqs. (28) and (29) so that the continuum limit is taken safely without spoiling the signum function approximation. All values for $p_{1,1}$ we evaluated numerically are tabulated in Appendix B. Figure 9 shows the cut-off $a/L$ dependence of $p_{1,1} + (1/12\pi^2)\ln(L/a)$ with $N_5 = 8$. We observe a similar cut-off dependence for the data with $N_5 = 16$ and 32.

We first validate the one-loop beta function $s_0$ by fitting $p_{1,1}$ as a function of

$1/N_S$ assuming the asymptotic form (49) including up to $O((a/L)^2)$ terms. All $r_k$ and $s_k$ are taken to be free parameters to validate the one-loop beta function $s_0$. We vary the cut-off $a/L = 1/N_S$ of the fit range $[0 : a/L]$ and investigate the stability on the fit result for $s_0$. We observe the stability in a asymptotic region and $s_0$ is consistent with the universal one-loop beta function within 10% accuracy with most MDWF actions we tested except for the case with the optimal Chiu type ($b_j = c_j$) with $N_5 = 8$. The discrepancy of $s_0$ with the optimal Chiu type ($b_j = c_j$) with $N_5 = 8$ is 20%.

We suppose the reason of the discrepancy with the optimal Chiu domain wall fermion with $N_5 = 8$ as follows. We employ $x \in [0.01 : 7.0]$ for the approximation range for the quasi optimal coefficient $b_j$ for the overlap type kernel $\mathcal{H}_W = \gamma_5 D_W$. The spectrum of the overlap kernel behaves as Eq. (29) and this limits the largest lattice size at $N_S = 72$. This case has a large $O(a)$ error coming from the explicit chiral symmetry breaking and the asymptotic behavior to extract the logarithmic cut-off dependence is not captured with the narrow fit range. To extend the fit range towards the asymptotic region in $a/L \to 0$ we need to decrease the lower limit of the approximation range. For the cases of the optimal Chiu MDWF with $N_5 = 16$ and 32, the effect of the explicit chiral symmetry breaking is suppressed so that the logarithmic divergence is captured in the fit ranges we examined.

To further check the universality of the MDWF in the SF scheme, we convert the coupling in the SF scheme to the coupling in the $\overline{\rm MS}$ scheme. The one-loop relation between the two schemes is known[59] as

$$\alpha_{\overline{\rm MS}}(\mu) = \alpha_{\rm SF}(\mu)\left[1 + c_1\alpha_{\rm SF}(\mu) + \cdots\right], \quad \mu = 1/L, \tag{50}$$

$$c_1 = c_{1,0} + N_f c_{1,1}, \tag{51}$$

$$c_{1,0} = 1.25563(4), \quad c_{1,1} = \begin{cases} 0.039863(2) & \text{for} \quad \theta = \pi/5 \\ 0.022504(2) & \text{for} \quad \theta = 0 \end{cases}, \tag{52}$$

where the fermionic contribution is $c_{1,1}$. This relation is universal and independent from the regularization used in the SF scheme. We employ the lattice regularization with the MDWF in the SF scheme and have the one-loop relation between the lattice bare coupling and the coupling renormalized with the SF scheme as Eq. (47). To extract $c_{1,1}$ from $r_0$, we have to know the one-loop relation between the lattice bare coupling with the MDWF and the coupling renormalized with the $\overline{\rm MS}$ scheme.

The MDWF action with $b_j + c_j = w_j, b_j - c_j = 1$ (optimal Shamir domain wall fermion) is equivalent to the standard domain wall fermion action in the infinite size of $N_5$. Therefore $r_0$ is expected to have a common value between the lattice fermions at $N_5 = \infty$. The one-loop relation between the lattice bare coupling with the standard domain wall fermion at $N_5 = \infty$ and $\alpha_{\overline{\rm MS}}$ has been obtained in Ref. 60. By combining the universal relation (50) and the results from Ref. 60, we expect $r_0 = 0.0010886(51)$ at $am_0 = 1.0$ and $r_0 = -0.0026362(33)$ at $am_0 = 1.5$ in $N_5 \to \infty$ for the optimal Shamir domain wall fermion.

Similarly the optimal Chiu DWF ($b_j = c_j = w_j$) and Boriçi DWF ($b_j = c_j = 1$)

Table 4. Fit results for $r_0$. $s_0$ is fixed at $-1/(12\pi^2)$. The values in the bottom row ($N_5 = \infty$) are estimated from the universal relation between the couplings in the SF and $\overline{\rm MS}$ schemes, and the relation between the coupling in the $\overline{\rm MS}$ scheme and in lattice bare coupling scheme with the standard domain wall fermion at $N_5 = \infty$ and with the overlap fermion.

| $m_0$ | 1.0 | | | 1.5 | |
|---|---|---|---|---|---|
| $N_5$ | $b_j + c_j = w_j$, $b_j - c_j = 1$ | $b_j = c_j = 1$ | $b_j = c_j = w_j$ | $b_j = 1, c_j = 0$ | $b_j = c_j = 1$ |
| 8 | −0.00100(18) | 0.010952(9) | – | −0.00373594(6) | 0.011679(5) |
| 16 | 0.001076(15) | 0.01116(3) | 0.01103(15) | −0.0026696(16) | 0.01184(15) |
| 32 | – | 0.01116(4) | 0.0111661(18) | −0.002634(2) | 0.01181(4) |
| $\infty$ | 0.0010886(51) | 0.011185(1) | | −0.0026362(33) | 0.011912(3) |

at $N_5 = \infty$ are equivalent to the overlap fermion action. $r_0$ is expected to have the same value as that derived from the overlap fermion. In Appendix C, we show the equivalence of $p_{1,1}$ between the MDWF and the overlap fermion algebraically. Using the one-loop relation between the lattice bare coupling with the overlap fermion and $\alpha_{\overline{\rm MS}}$ obtained in Ref. 61, we expect $r_0 = 0.01118458(16)$ at $am_0 = 1.0$ and $r_0 = 0.01191070(16)$ at $am_0 = 1.5$ for the MDWF with $b_j = c_j$ at $N_5 = \infty$.

We fit $p_{1,1}$ with Eq. (49) with fixing $s_0 = -1/(12\pi^2)$ to extract $r_0$. We exclude the optimal Chiu DWF with $N_5 = 8$ from the analysis as we failed the validation on $s_0$ with the fit analysis without any constraints. We employ three fit functions to estimate $r_0$,

$$f(x) = r_0^f + s_0 \ln(x) + (r_1^f + s_1^g \ln(x))/x, \tag{53}$$

$$p(x) = r_0^p + s_0 \ln(x) + (r_1^p + s_1^p \ln(x))/x + (r_2^p + s_2^p \ln(x))/x^2, \tag{54}$$

$$r(x) = r_0^r + s_0 \ln(x) + (r_1^r + s_1^r \ln(x))/x + (r_2^r + s_2^r \ln(x))/x^2 + (r_2^r + s_2^r \ln(x))/x^3, \tag{55}$$

where $x = L/a$. Table 4 shows the fit results for $r_0$, where the error is estimated from the stability on the fit results by varying the fit range and by changing the fitting function. We confirm that $r_0$'s agree with the expected values for sufficiently large $N_5$. From these observations on $s_0$ and $r_0$, we conclude that the MDWF with the boundary term Eq. (22) actuary satisfies the desired universality at $N_5 = \infty$.

To further confirm our construction of the MDWF with the SF scheme, we need to validate $r_0$ at a small $N_5$. This requires an independent computation of the one-loop relation between the lattice bare coupling with the MDWF at a small $N_5$ and the coupling in the $\overline{\rm MS}$ scheme as has been done in Refs. 60, 61.

We next evaluate the effect of the $O(a)$ improvement by the boundary coefficient $c_{\rm SF}$. The lattice chiral symmetry is explicitly broken in the cases with smaller $N_5$, which causes $O(a)$ errors that cannot be removed by the boundary improvement. To remove the $O(a)$ errors from the explicit breaking of the lattice chiral symmetry, the clover term must be included and adjusted. To see the effect of the boundary improvement we investigate the cases where $r_0$ is consistent with the value at $N_5 = \infty$. These cases are expected to have numerically exact lattice chiral symmetry and

Table 5. Fit results for $s_1$. $s_0$ is fixed at $-1/(12\pi^2)$ and $r_0$ are fixed at the universal values at $N_5 = \infty$.

| $m_0$ | 1.0 | | | 1.5 | |
|---|---|---|---|---|---|
| $N_5$ | $b_j + c_j = w_j$, $b_j - c_j = 1$ | $b_j = c_j = 1$ | $b_j = c_j = w_j$ | $b_j = 1, c_j = 0$ | $b_j = c_j = 1$ |
| 16 | −0.00115(3) | 0.00116(6) | −0.0080(7) | – | 0.0041(13) |
| 32 | – | 0.00112(4) | −0.00490(3) | −0.0014(2) | 0.0038(9) |

no $O(a)$ error except from that induced by the boundary term.

Table 5 shows the fit results for $s_1$, which is expected to be zero when $c_{\rm SF}$ is properly tuned. We fit $p_{1,1}$ with

$$f(x) = r_0 + s_0 \ln(x) + (r_1^f + s_1^g \ln(x))/x, \tag{56}$$

$$p(x) = r_0 + s_0 \ln(x) + (r_1^p + s_1^p \ln(x))/x + (r_2^p + s_2^p \ln(x))/x^2, \tag{57}$$

where $s_0$ and $r_0$ are fixed to the universal values. The error on $s_1$ is estimated as has been done for $r_0$. The values are close to zero but slightly deviates from zero. The reason of the deviation from zero is that there still remains the explicit lattice chiral symmetry breaking at these finite $N_5$ or the miss-tuning of $c_{\rm SF}$. To confirm the $O(a)$ improvement more precisely we need more data of $p_{1,1}$ at larger $L/a$ to stabilize the fitting to the asymptotic form.

## 7. Conclusion

We have constructed the appropriate boundary operator for the Möbius domain wall fermions (MDWF) to define the Schrödinger functional (SF) scheme by extending the Takeda's formulation which is done for the standard domain wall fermion.

We investigated the effective four-dimensional operator derived from the MDWF at the tree-level and confirmed that the spectrum and the propagator reproduce the continuum behavior in the continuum limit. We observed the propagator touching the boundary surfaces needs a renormalization at the tree-level. This requires counter terms to the surface fermion fields. However we did not find appropriate counter term analytically. The surface field renormalization seems to be irrelevant in the continuum limit. The surface field renormalization could be absorbed in to the renormalization of the boundary operator.

We investigated the fermionic contribution to the one-loop beta function, $p_{1,1}$, with the MDWF using the several parameter sets. We could extract the one-loop beta function consistent with the universal value within a 10% difference for the most of the parameter sets. The one exception was the case with the optimal Chiu domain wall fermion with $N_5 = 8$, which has a 20% deviation from the universal one-loop beta function. The universal relation of the couplings between the SF scheme and $\overline{\rm MS}$ scheme was examined and we found that the cases with sufficiently larger $N_5$ were consistent with the known values from the standard domain wall fermion and the overlap fermion. To validate the universality of the coupling relation between

the SF and $\overline{\rm MS}$ schemes with the MDWF at smaller $N_5$, another validation using the relation between the $\overline{\rm MS}$ coupling and the bare lattice coupling with the MDWF is required.

We conclude that the boundary operator we introduced is one of the realization of the SF scheme for the Möbius domain wall fermions, at least at a larger $N_5$ or $N_5 = \infty$.

## Acknowledgments

We would like to thank S. Takeda for the computational advice and the useful discussion. The numerical computations have been done on the workstations of the INSAM (Institute for Nonlinear Sciences and Applied Mathematics) at Hiroshima University and on FUJITSU PRIMERGY CX400 (Tatara system) of the Research Institute for Information Technology at Kyushu University. This work was partly supported by JSPS KAKENHI Grant Numbers 24540276 and 16K05326, and Core of Research for the Energetic Universe (CORE–U) at Hiroshima University.

## Appendix A. Tables for quasi optimal parameters $b_j$

In this appendix we list the quasi optimal parameters $b_j$ for $N_5 = 8, 16$ and 32 cases. The approximation range is fixed to $x \in [0.001 : 1.00]$ for the optimal Shamir domain wall fermion (OSDWF, $b_j + c_j = w_j, b_j - c_j = 1$), and $x \in [0.01 : 7.00]$ for the optimal Chiu domain wall fermion (OCDWF, $b_j = c_j = w_j$). We introduce $\delta^{N_5} = |1 - R_{N_5}|$ to see the quality of the approximation.

Table A1. The MDWF parameters $b_j$.

| OSDWF | | | |
|---|---|---|---|
| $N_5$ | 8 | 16 | 32 |
| $\delta^{N_5}$ | $\leq 0.091$ | $\leq 0.00061$ | $\leq 4.3 \times 10^{-8}$ |
| $j$ | | $b_j$ | |
| 1 | 1.375560445952 | 1.070238032009 | 0.016892137272 |
| 2 | 5.471160816064 | 1.730342867161 | 0.158913006904 |
| 3 | 50.79006488628 | 3.876257791467 | 0.482041690426 |
| 4 | 286.0314000944 | 9.868218005280 | 1.074927835108 |
| 5 | | 27.18597163933 | 2.100739142300 |
| 6 | | 74.54647850997 | 3.840873748406 |
| 7 | | 203.6953910351 | 6.774084261660 |
| 8 | | 438.9134097812 | 11.70429696596 |
| 9 | | | 19.98458839515 |
| 10 | | | 33.86858730352 |
| 11 | | | 57.09209193583 |
| 12 | | | 95.62651877838 |
| 13 | | | 158.2374319172 |
| 14 | | | 254.0716769840 |
| 15 | | | 378.9127561311 |
| 16 | | | 483.1599011152 |

| OCDWF | | | |
|---|---|---|---|
| $N_5$ | 8 | 16 | 32 |
| $\delta^{N_5}$ | $\leq 0.072$ | $\leq 0.00039$ | $\leq 1.8 \times 10^{-8}$ |
| $j$ | | $b_j$ | |
| 1 | 0.237921110807 | 0.161123304598 | 0.147274921719 |
| 2 | 1.265028710883 | 0.331200294113 | 0.184266408796 |
| 3 | 11.292798466011 | 0.862987775592 | 0.267551476942 |
| 4 | 60.043912191189 | 2.293352637899 | 0.418026489555 |
| 5 | | 6.229183445073 | 0.673528275619 |
| 6 | | 16.553785221249 | 1.098151069375 |
| 7 | | 43.133157003882 | 1.798613861602 |
| 8 | | 88.663240375751 | 2.950400432880 |
| 9 | | | 4.841957764956 |
| 10 | | | 7.942624367962 |
| 11 | | | 13.008878909391 |
| 12 | | | 21.210266595825 |
| 13 | | | 34.174184274611 |
| 14 | | | 53.394264344831 |
| 15 | | | 77.527501507451 |
| 16 | | | 97.000318309165 |

## Appendix B. Tables for $p_{1,1}$

In this appendix we accumulate tables for the numerical values of $p_{1,1}$.

Table B1. The numerical values for $p_{1,1}$ with $b_j + c_j = w_j, b_j - c_j = 1$ and $m_0 = 1.0$.

| $N_5$ | 8 | 16 |
|---|---|---|
| $L/a$ | $p_{1,1}$ | |
| 4 | −0.008078678483014 | −0.007549846131326 |
| 6 | −0.012704626284028 | −0.011543790007817 |
| 8 | −0.016099359107337 | −0.014362647277993 |
| 10 | −0.018603053000762 | −0.016601560471003 |
| 12 | −0.020509350351466 | −0.018419096227329 |
| 14 | −0.022043043374366 | −0.019932682101795 |
| 16 | −0.023334785689534 | −0.021224758101492 |
| 18 | −0.024458027530347 | −0.022349705318640 |
| 20 | −0.025455706039567 | −0.023344258955488 |
| 22 | −0.026354442980561 | −0.024234463201614 |
| 24 | −0.027171888915236 | −0.025039552752149 |
| 26 | −0.027920587948598 | −0.025774134656849 |
| 28 | −0.028610040120546 | −0.026449513032584 |
| 30 | −0.029247813609523 | −0.027074562214969 |
| 32 | −0.029840155519369 | −0.027656336722746 |
| 34 | −0.030392340093947 | −0.028200511774470 |
| 36 | −0.030908880213565 | −0.028711707029837 |
| 38 | −0.031393667187825 | −0.029193726826378 |
| 40 | −0.031850071712519 | −0.029649739643784 |
| 42 | −0.032281022324532 | −0.030082412981785 |
| 44 | −0.032689069460135 | −0.030494015386321 |
| 46 | −0.033076439227606 | −0.030886494192633 |
| 48 | −0.033445079148571 | −0.031261535256350 |
| 50 | −0.033796697257952 | |
| 52 | −0.034132795554748 | |
| 54 | −0.034454698597199 | |
| 56 | −0.034763577918903 | |
| 58 | −0.035060472857527 | |
| 60 | −0.035346308315376 | |
| 62 | −0.035621909905414 | |
| 64 | −0.035888016875790 | |
| 66 | −0.036145293150457 | |
| 68 | −0.036394336774732 | |
| 70 | −0.036635688010451 | |
| 72 | −0.036869836288573 | |
| 74 | −0.037097226193355 | |
| 76 | −0.037318262626538 | |
| 78 | −0.037533315274019 | |
| 80 | −0.037742722480864 | |

Table B2. Same as Table B1, but with $b_j = c_j = w_j$ and $m_0 = 1.0$.

| $N_5$ | 8 | 16 | 32 |
|---|---|---|---|
| $L/a$ | | $p_{1,1}$ | |
| 4 | −0.000427658644074 | −0.000383843417187 | −0.001367108292250 |
| 6 | −0.001690115887320 | −0.002015195493540 | −0.003292843399314 |
| 8 | −0.003276057963329 | −0.004212644775318 | −0.005485336972469 |
| 10 | −0.005033155003610 | −0.006246918403858 | −0.007449843475257 |
| 12 | −0.006705005271095 | −0.007992466113233 | −0.009112723836382 |
| 14 | −0.008193831514685 | −0.009490189069814 | −0.010524786720790 |
| 16 | −0.009494057300111 | −0.010790678620702 | −0.011742834419345 |
| 18 | −0.010630559779250 | −0.011933438152156 | −0.012810419169036 |
| 20 | −0.011632825706636 | −0.012948842121387 | −0.013759177135561 |
| 22 | −0.012526885001577 | −0.013860522358465 | −0.014612217134086 |
| 24 | −0.013333735423218 | −0.014686861614616 | −0.015386734394376 |
| 26 | −0.014069766215183 | −0.015442121609423 | −0.016095786578485 |
| 28 | −0.014747628848984 | −0.016137387857025 | −0.016749483310047 |
| 30 | −0.015377075017193 | −0.016781345974691 | −0.017355791924810 |
| 32 | −0.015965645179162 | −0.017380889556003 | −0.017921092828360 |
| 34 | −0.016519204136393 | −0.017941576933597 | −0.018450569412746 |
| 36 | −0.017042349063875 | −0.018467964970409 | −0.018948486893592 |
| 38 | −0.017538717989105 | −0.018963849305390 | −0.019418395305982 |
| 40 | −0.018011222352760 | −0.019432436525828 | −0.019863279824302 |
| 42 | −0.018462222102058 | −0.019876468167950 | −0.020285673857459 |
| 44 | −0.018893657364280 | −0.020298311160125 | −0.020687745384951 |
| 46 | −0.019307147334419 | −0.020700025025448 | −0.021071363741383 |
| 48 | −0.019704064430391 | −0.021083412945066 | −0.021438151897327 |
| 50 | −0.020085589825083 | −0.021450061496227 | |
| 52 | −0.020452754991647 | −0.021801372306609 | |
| 54 | −0.020806472777243 | −0.022138587806451 | |
| 56 | −0.021147560664753 | −0.022462812558580 | |
| 58 | −0.021476758226712 | −0.022775031183158 | |
| 60 | −0.021794740276988 | −0.023076123590416 | |
| 62 | −0.022102126845674 | −0.023366878034668 | |
| 64 | −0.022399490814134 | −0.023648002369445 | |
| 66 | −0.022687363830450 | −0.023920133794130 | |
| 68 | −0.022966240962226 | −0.024183847319741 | |
| 70 | −0.023236584421461 | −0.024439663137563 | |

Table B3. Same as Table B1, but with $b_j = 1, c_j = 0$ and $m_0 = 1.5$.

| $N_5$ | 8 | 16 | 32 |
|---|---|---|---|
| $L/a$ | | $p_{1,1}$ | |
| 4 | −0.013700543988949 | −0.013494117365375 | −0.013493847599046 |
| 6 | −0.016940425660898 | −0.016440093560490 | −0.016435046256293 |
| 8 | −0.019207595711335 | −0.018495725966135 | −0.018480529959025 |
| 10 | −0.021308125813259 | −0.020479834297536 | −0.020459083387075 |
| 12 | −0.023122800312741 | −0.022221285948861 | −0.022198883266909 |
| 14 | −0.024665375229509 | −0.023711578334847 | −0.023688561490842 |
| 16 | −0.025987047538505 | −0.024995171537818 | −0.024971355383199 |
| 18 | −0.027135213800013 | −0.026116105185960 | −0.026091198129590 |
| 20 | −0.028146880041840 | −0.027108518882633 | −0.027082437011268 |
| 22 | −0.029049775493944 | −0.027997747140651 | −0.027970577120069 |
| 24 | −0.029864559491185 | −0.028802679063304 | −0.028774578712134 |
| 26 | −0.030606757871299 | −0.029537633821171 | −0.029508765297232 |
| 28 | −0.031288217026821 | −0.030213664582947 | −0.030184166135890 |
| 30 | −0.031918135064723 | −0.030839449899792 | −0.030809430378576 |
| 32 | −0.032503778953037 | −0.031421910597608 | −0.031391453294570 |
| 34 | −0.033050983428172 | −0.031966644411249 | −0.031935813074617 |
| 36 | −0.033564501913902 | −0.032478237562439 | −0.032447081752874 |
| 38 | −0.034048257349549 | −0.032960491706605 | −0.032929050814620 |
| 40 | −0.034505524685294 | −0.033416591708052 | −0.033384897755921 |
| 42 | −0.034939066008357 | −0.033849231429220 | −0.033817310976307 |
| 44 | −0.035351232253616 | −0.034260709315154 | −0.034228584756533 |
| 46 | −0.035744040922304 | −0.034653001956654 | −0.034620692426401 |
| 48 | −0.036119236284169 | −0.035027821389594 | −0.034995343407687 |

Table B4. Same as Table B1, but with $b_j = c_j = 1$ and $m_0 = 1.5$.

| $N_5$ | 8 | 16 | 32 |
|---|---|---|---|
| $L/a$ | | $p_{1,1}$ | |
| 4 | −0.006727819825856 | −0.006665138308415 | −0.006666313597976 |
| 6 | −0.007414851979212 | −0.007313811347951 | −0.007315034976460 |
| 8 | −0.008380305729795 | −0.008194515940394 | −0.008185897962635 |
| 10 | −0.009706986889307 | −0.009534951147513 | −0.009513426996691 |
| 12 | −0.010940734313774 | −0.010849913953446 | −0.010828496014809 |
| 14 | −0.012005880912213 | −0.012000303082120 | −0.011989158728680 |
| 16 | −0.012933090094362 | −0.012990681811199 | −0.012992846763797 |
| 18 | −0.013759688673405 | −0.013854127110319 | −0.013868798328790 |
| 20 | −0.014511760217989 | −0.014620713721791 | −0.014645831748636 |
| 22 | −0.015205517755086 | −0.015312808751915 | −0.015346126770424 |
| 24 | −0.015851036926812 | −0.015946323963520 | −0.015985730259767 |
| 26 | −0.016454984507842 | −0.016532563270011 | −0.016576163504983 |
| 28 | −0.017022194974289 | −0.017079658119618 | −0.017125805557620 |
| 30 | −0.017556489774245 | −0.017593563907684 | −0.017640879135091 |
| 32 | −0.018061078280186 | −0.018078737359153 | −0.018126116251055 |
| 34 | −0.018538749124392 | −0.018538597095271 | −0.018585202424702 |
| 36 | −0.018991964014254 | −0.018975837134752 | −0.019021074631616 |
| 38 | −0.019422909145805 | −0.019392639865905 | −0.019436123561516 |
| 40 | −0.019833529265709 | −0.019790820185260 | −0.019832332961955 |
| 42 | −0.020225554783800 | −0.020171922778777 | −0.020211377175424 |
| 44 | −0.020600525735608 | −0.020537287838630 | −0.020574690536960 |
| 46 | −0.020959813694587 | −0.020888095769654 | −0.020923517571072 |
| 48 | −0.021304641794774 | −0.021225398065531 | −0.021258949911228 |
| 50 | −0.021636102804375 | | |
| 52 | −0.021955175221099 | | |
| 54 | −0.022262737442725 | | |
| 56 | −0.022559580138765 | | |
| 58 | −0.022846416992679 | | |
| 60 | −0.023123893996791 | | |
| 62 | −0.023392597486309 | | |
| 64 | −0.023653061081057 | | |
| 66 | −0.023905771690838 | | |
| 68 | −0.024151174719892 | | |
| 70 | −0.024389678584948 | | |
| 72 | −0.024621658651276 | | |
| 74 | −0.024847460666186 | | |
| 76 | −0.025067403767381 | | |
| 78 | −0.025281783121781 | | |
| 80 | −0.025490872250634 | | |

Table B5. Same as Table B1, but with $b_j = c_j = 1$ and $m_0 = 1.0$.

| $N_5$ | 8 | 16 | 32 |
|---|---|---|---|
| $L/a$ | | $p_{1,1}$ | |
| 4 | −0.000996246152616 | −0.000931659891244 | −0.000931919758575 |
| 6 | −0.004603150636507 | −0.004379720711230 | −0.004377564445862 |
| 8 | −0.007570846735406 | −0.007339903403487 | −0.007334795622206 |
| 10 | −0.009663145567390 | −0.009487128771071 | −0.009482501467147 |
| 12 | −0.011187581989197 | −0.011061057467551 | −0.011058231188890 |
| 14 | −0.012384896118215 | −0.012290534341752 | −0.012289409163346 |
| 16 | −0.013389461252875 | −0.013310783001584 | −0.013310976363075 |
| 18 | −0.014270981623373 | −0.014195328866723 | −0.014196493673909 |
| 20 | −0.015065582916720 | −0.014984779892570 | −0.014986622226234 |
| 22 | −0.015792971302519 | −0.015702711408268 | −0.015704971170587 |
| 24 | −0.016465000994347 | −0.016363707733056 | −0.016366158318439 |
| 26 | −0.017089703923897 | −0.016977430784739 | −0.016979889094112 |
| 28 | −0.017673114155514 | −0.017550726401246 | −0.017553059566649 |
| 30 | −0.018220085378664 | −0.018088745432749 | −0.018090869408541 |
| 32 | −0.018734670587965 | −0.018595557661083 | −0.018597429341229 |
| 34 | −0.019220317416919 | −0.019074498753218 | −0.019076105281324 |
| 36 | −0.019679985859805 | −0.019528374164715 | −0.019529722477420 |
| 38 | −0.020116231188214 | −0.019959585129973 | −0.019960693392692 |
| 40 | −0.020531268659271 | −0.020370211346101 | −0.020371102773105 |
| 42 | −0.020927026511223 | −0.020762068840545 | −0.020762767700268 |
| 44 | −0.021305190093525 | −0.021136752957334 | −0.021137282277683 |
| 46 | −0.021667238733567 | −0.021495671861383 | −0.021496052316441 |
| 48 | −0.022014476511803 | −0.021840073569361 | −0.021840323109700 |

## Appendix C. Equivalence of the fermionic contribution $p_{1,1}$ between the five-dimensional operator and the effective four-dimensional operator

In this appendix we prove the equivalence of $p_{1,1}$ constructed with the MDWF and with the effective four-dimensional operators.

The fermionic contribution $p_{1,1}$ is defined by

$$\begin{aligned} p_{1,1} &= \frac{1}{k}\frac{\partial}{\partial\eta}\left[\mathrm{Tr}\ln\left[Z^{-1}D_{PV}^{-1}D_{\mathrm{MDWF}}\right]\right] \\ &= \frac{1}{k}\mathrm{Tr}\left[\frac{\partial D_{\mathrm{MDWF}}}{\partial\eta}(D_{\mathrm{MDWF}})^{-1} - \frac{\partial D_{\mathrm{PV}}}{\partial\eta}(D_{\mathrm{PV}})^{-1}\right], \end{aligned} \tag{C.1}$$

with the MDWF operator in the five-dimensional lattice. The trace is taken on the five-dimensional lattice sites, color, and spinor indexes. Eq. (48) is the momentum space representation of Eq. (C.1). We omit the superscript $N_5$ and substitution of $\eta = 0$ after the differentiation with $\eta$ for simplicity in this appendix.

The one-loop contribution to the effective action with the effective four-

dimensional operator is

$$p_{1,1}^{\text{eff}} = \frac{1}{k}\frac{\partial}{\partial\eta}\Big[\text{tr}\ln\left[D_q\right]\Big], \tag{C.2}$$

where $D_q$ is defined in Eq. (27), and the trace is taken on the four-dimensional lattice sites, color, and spinor indexes. The effective four-dimensional operator is renormalized by $Z$ and $am_{\text{res}}$ according to Eqs. (27), (18), and (19). We show $p_{1,1} = p_{1,1}^{\text{eff}}$ in the following.

Substituting Eqs. (8) and (27) into Eq. (C.2), we have

$$p_{1,1}^{\text{eff}} = \frac{1}{k}\text{tr}\left[\epsilon^T P^T (D_{\text{MDWF}})^{-1} D_{\text{PV}} P\epsilon \right. \\ \left. \times\ \epsilon^T P^T \left\{-(D_{\text{PV}})^{-1}\frac{\partial D_{\text{PV}}}{\partial\eta} D_{\text{PV}}^{-1} D_{\text{MDWF}} + (D_{\text{PV}})^{-1}\frac{\partial D_{\text{MDWF}}}{\partial\eta}\right\} P\epsilon\right]. \tag{C.3}$$

We introduce two matrices $A$ and $B$ defined by

$$A = P^T (D_{\text{MDWF}})^{-1} D_{\text{PV}} P, \tag{C.4}$$

$$B = P^T \left\{(D_{\text{PV}})^{-1}\frac{\partial D_{\text{MDWF}}}{\partial\eta} - (D_{\text{PV}})^{-1}\frac{\partial D_{\text{PV}}}{\partial\eta}(D_{\text{PV}})^{-1} D_{\text{MDWF}}\right\} P. \tag{C.5}$$

to simplify $p_{1,1}$ and $p_{1,1}^{\text{eff}}$ as

$$p_{1,1} = \frac{1}{k}\text{Tr}\left[AB\right], \tag{C.6}$$

$$p_{1,1}^{\text{eff}} = \frac{1}{k}\text{tr}\left[(\epsilon^T A\epsilon)\ (\epsilon^T B\epsilon)\right], \tag{C.7}$$

where $PP^T = 1$ is used.

After some matrix algebra in the five-dimensional notation, we obtain

$$A = \left(\begin{array}{c|c} 1-(1-m_f)\alpha & 0 \\ \hline \vec{z} & \boldsymbol{I} \end{array}\right), \tag{C.8}$$

$$B = \left(\begin{array}{c|c} \gamma & 0 \\ \hline \vec{g} & \mathbf{0} \end{array}\right), \tag{C.9}$$

where $\alpha$ and $\gamma$ are four-dimensional operators, and $\vec{z}$ and $\vec{g}$ contain $N_5 - 1$ four-dimensional operators. Their explicit forms are not required in the proof.

Substituting Eqs. (C.8) and (C.9) into Eq. (C.6), we obtain

$$p_{1,1} = \frac{1}{k}\mathrm{Tr}\left[\left(\begin{array}{c|c} 1-(1-m_f)\alpha & 0 \\ \hline \overrightarrow{z} & \boldsymbol{I} \end{array}\right)\left(\begin{array}{c|c} \gamma & 0 \\ \hline \overrightarrow{g} & \mathbf{0} \end{array}\right)\right]$$

$$= \frac{1}{k}\mathrm{tr}[\{1-(1-m_f)\alpha\}\gamma], \tag{C.10}$$

where the trace in the last line is now taken only on the four-dimensional lattice, color, and spinor indexes.

Similarly substituting Eqs. (C.8) and (C.9) into Eq. (C.7), we obtain

$$p_{1,1}^{\mathrm{eff}} = \frac{1}{k}\mathrm{Tr}\left[\begin{pmatrix}1 & 0 & \cdots & 0\end{pmatrix}\left(\begin{array}{c|c} 1-(1-m_f)\alpha & 0 \\ \hline \overrightarrow{z} & \boldsymbol{I} \end{array}\right)\begin{pmatrix}1\\0\\\vdots\\0\end{pmatrix}\right.$$

$$\left.\times\begin{pmatrix}1 & 0 & \cdots & 0\end{pmatrix}\left(\begin{array}{c|c} \gamma & 0 \\ \hline \overrightarrow{g} & \mathbf{0} \end{array}\right)\begin{pmatrix}1\\0\\\vdots\\0\end{pmatrix}\right]$$

$$= \frac{1}{k}\mathrm{tr}[\{1-(1-m_f)\alpha\}\gamma]. \tag{C.11}$$

Thus we have proved $p_{1,1} = p_{1,1}^{\mathrm{eff}}$.

We also note that

$$(D_q)^{-1} = \epsilon^T P^T (D_{\mathrm{MDWF}})^{-1} D_{\mathrm{PV}} P \epsilon, \tag{C.12}$$

holds even with the SF boundary term.

## References

1. P. Hasenfratz, Nucl. Phys. B **525**, 401 (1998) [hep-lat/9802007].
2. P. Hasenfratz, V. Laliena and F. Niedermayer, Phys. Lett. B **427**, 125 (1998) [hep-lat/9801021].
3. D. B. Kaplan, Phys. Lett. B **288**, 342 (1992) [hep-lat/9206013].
4. R. Narayanan and H. Neuberger, Phys. Lett. B **302**, 62 (1993) [hep-lat/9212019].
5. R. Narayanan and H. Neuberger, Phys. Rev. Lett. **71**, 3251 (1993) [hep-lat/9308011].
6. R. Narayanan and H. Neuberger, Nucl. Phys. B **412**, 574 (1994) [hep-lat/9307006].
7. P. H. Ginsparg and K. G. Wilson, Phys. Rev. D **25**, 2649 (1982).
8. M. Lüscher, Phys. Lett. B **428**, 342 (1998) [hep-lat/9802011].
9. M. Creutz, Rev. Mod. Phys. **73**, 119 (2001) [hep-lat/0007032].
10. H. Neuberger, Ann. Rev. Nucl. Part. Sci. **51**, 23 (2001) [hep-lat/0101006].
11. S. Chandrasekharan and U. J. Wiese, Prog. Part. Nucl. Phys. **53**, 373 (2004) [hep-lat/0405024].

12. For a review on the recent lattice QCD results, see : S. Aoki, Y. Aoki, C. Bernard, T. Blum, G. Colangelo, M. Della Morte, S. Dürr and A. X. El Khadra *et al.*, Eur. Phys. J. C **74**, no. 9, 2890 (2014) [arXiv:1310.8555 [hep-lat]], and references therein.
13. G. Martinelli, S. Petrarca, C. T. Sachrajda and A. Vladikas, Phys. Lett. B **311**, 241 (1993) [Erratum-ibid. B **317**, 660 (1993)].
14. G. Martinelli, C. Pittori, C. T. Sachrajda, M. Testa and A. Vladikas, Nucl. Phys. B **445**, 81 (1995) [hep-lat/9411010].
15. M. Lüscher, R. Narayanan, P. Weisz and U. Wolff, Nucl. Phys. B **384**, 168 (1992) [hep-lat/9207009].
16. S. Sint, Nucl. Phys. B **421**, 135 (1994) [hep-lat/9312079].
17. M. Lüscher, R. Sommer, P. Weisz and U. Wolff, Nucl. Phys. B **413**, 481 (1994) [hep-lat/9309005].
18. S. Sint, Nucl. Phys. B **451**, 416 (1995) [hep-lat/9504005].
19. M. Lüscher, JHEP **1008**, 071 (2010) [Erratum-ibid. **1403**, 092 (2014)] [arXiv:1006.4518 [hep-lat]].
20. M. Lüscher and P. Weisz, JHEP **1102**, 051 (2011) [arXiv:1101.0963 [hep-th]].
21. Z. Fodor, K. Holland, J. Kuti, D. Nogradi and C. H. Wong, JHEP **1211**, 007 (2012) [arXiv:1208.1051 [hep-lat]].
22. P. Fritzsch and A. Ramos, JHEP **1310**, 008 (2013) [arXiv:1301.4388 [hep-lat]].
23. H. Suzuki, PTEP **2013**, no. 8, 083B03 (2013) [arXiv:1304.0533 [hep-lat]].
24. M. Lüscher, JHEP **1304**, 123 (2013) [arXiv:1302.5246 [hep-lat]].
25. M. Lüscher and P. Weisz, Nucl. Phys. B **479**, 429 (1996) [hep-lat/9606016].
26. M. Lüscher, S. Sint, R. Sommer, P. Weisz and U. Wolff, Nucl. Phys. B **491**, 323 (1997) [hep-lat/9609035].
27. M. Lüscher, S. Sint, R. Sommer and H. Wittig, Nucl. Phys. B **491**, 344 (1997) [hep-lat/9611015].
28. K. Jansen *et al.* [ALPHA Collaboration], Nucl. Phys. B **530**, 185 (1998) [Erratum-ibid. B **643**, 517 (2002)] [hep-lat/9803017].
29. S. Capitani *et al.* [ALPHA Collaboration], Nucl. Phys. B **544**, 669 (1999) [hep-lat/9810063].
30. S. Sint *et al.* [ALPHA Collaboration], Nucl. Phys. B **545**, 529 (1999) [hep-lat/9808013].
31. A. Bode *et al.* [ALPHA Collaboration], Phys. Lett. B **515**, 49 (2001) [hep-lat/0105003].
32. M. Della Morte *et al.* [ALPHA Collaboration], Nucl. Phys. B **713**, 378 (2005) [hep-lat/0411025].
33. M. Guagnelli *et al.* [ALPHA Collaboration], JHEP **0603**, 088 (2006) [hep-lat/0505002].
34. M. Della Morte *et al.* [ALPHA Collaboration], Nucl. Phys. B **729**, 117 (2005) [hep-lat/0507035].
35. P. Dimopoulos *et al.* [ALPHA Collaboration], JHEP **0805**, 065 (2008) [arXiv:0712.2429 [hep-lat]].
36. Y. Taniguchi, JHEP **0610**, 027 (2006) [hep-lat/0604002].
37. Y. Taniguchi, JHEP **0512**, 037 (2005) [hep-lat/0412024].
38. M. Lüscher, JHEP **0605**, 042 (2006) [hep-lat/0603029].
39. S. Sint, PoS LAT **2007**, 253 (2007).
40. S. Takeda, Nucl. Phys. B **796**, 402 (2008) [arXiv:0712.1469 [hep-lat]].
41. S. Takeda, Phys. Rev. D **87**, no. 11, 114506 (2013) [arXiv:1010.3504 [hep-lat]].
42. R. C. Brower, H. Neff and K. Orginos, Nucl. Phys. Proc. Suppl. **140**, 686 (2005) [hep-lat/0409118].
43. R. C. Brower, H. Neff and K. Orginos, arXiv:1206.5214 [hep-lat].
44. S. Hashimoto, S. Aoki, G. Cossu, H. Fukaya, T. Kaneko, J. Noaki and P. A. Boyle,

PoS LATTICE **2013**, 431 (2014).
45. Y. Murakami and K. I. Ishikawa, PoS LATTICE **2015** (2015) 308 [arXiv:1701.07139 [hep-lat]].
46. Y. Murakami and K. I. Ishikawa, arXiv:1410.8335 [hep-lat].
47. Y. Kikukawa and T. Noguchi, hep-lat/9902022.
48. S. Capitani, PoS LAT **2007**, 066 (2007) [arXiv:0708.3281 [hep-lat]].
49. A. Boriçi, Nucl. Phys. Proc. Suppl. **83** (2000) 771 [hep-lat/9909057].
50. A. Boriçi, in Lattice Fermions and Structure of the Vacuum, V. Mitrjushkin *et al.* (edts.), Springer 2000, [hep-lat/9912040].
51. A. Boriçi, in QCD and numerical analysis III, A. Boriçi *et al.* (edts.), Springer 2005, [hep-lat/0402035].
52. T. W. Chiu, Phys. Rev. Lett. **90**, 071601 (2003) [hep-lat/0209153].
53. V. Furman and Y. Shamir, Nucl. Phys. B **439**, 54 (1995) [hep-lat/9405004].
54. Y. C. Chen and T. W. Chiu, Phys. Lett. B **738**, 55 (2014) [arXiv:1403.1683 [hep-lat]].
55. K. Ogawa *et al.* [TWQCD Collaboration], PoS LAT **2009**, 033 (2009) [arXiv:0911.5532 [hep-lat]].
56. P. A. Boyle [UKQCD Collaboration], PoS LATTICE **2014** (2015) 087.
57. T. W. Chiu, Phys. Lett. B **744** (2015) 95 [arXiv:1503.01750 [hep-lat]].
58. T. W. Chiu, T. H. Hsieh, C. H. Huang and T. R. Huang, Phys. Rev. D **66**, 114502 (2002) [hep-lat/0206007].
59. S. Sint and R. Sommer, Nucl. Phys. B **465** (1996) 71 [hep-lat/9508012].
60. S. Aoki and Y. Kuramashi, Phys. Rev. D **68** (2003) 034507 [hep-lat/0306008].
61. C. Alexandrou, H. Panagopoulos and E. Vicari, Nucl. Phys. B **571** (2000) 257 [hep-lat/9909158].